Development of a Finite Element Model to Study the Torsional Fracture Strength of an Analogue Tibia with Bicortical Holes

K. Reuter[1], A. Chong[2], V. Madhavan[3], P. Wooley[2], M. Virginia[4], and H.M. Lankarani[3 *]

[1] *National Institute for Aviation research, Wichita State University, Wichita, Kansas, USA*
[2] *Orthopedic Research Institute, Wichita, Kansas, USA*
[3] *College of Engineering, Wichita State University, Wichita, Kanas, USA*
[4] *Altair Engineering, Wichita, Kansas, USA*
[*] (Corresponding Author)

Abstract

Fractured bones are often stabilized with orthopedic fracture plates and screws until healed. If the plates and screws are removed, the vacant screw holes introduce a potential site for re-fracture. This study is aimed at simulating a laboratory torsional fracture test of a composite analogue tibia with vacant screw holes using a finite element (FE) model. This FE model is set up the same as the experimental torsion test, with a section from the distal portion of the tibia. The FE model contains over 35k second-order brick elements and nearly 165k nodes. It utilizes an isotropic linear elastic material law with material properties obtained from the analogue tibia manufacturer. Comparisons between the experimental model and the FE model consider the fracture torque, fracture angle, and specific torsional stiffness. Stress contours of the FE model are compared to the fracture path of the experimental model. The FE model predicts the fracture location and a fracture torque within the standard deviation of that determined experimentally.

Keywords: Finite element modeling and analysis; Biomechanics; Composite; Human tibia; Failure strength; Torsion; Screw holes

Introduction

Plates and screws are common orthopedic devices used to stabilize fractured bones. When this hardware is removed, there is potential for re-fracture, especially under torsional loading, due to the reduction in torsional strength caused by the presence of vacant screw holes [1, 2, 3, 4, 5, 6].

Clinical interest in determining the risk of re-fracture after screw removal has led to experimental and finite element (FE) studies on the torsional fracture strength of long bones with holes [7, 8, 9, 10, 11]. The FE models used thus far analyze the geometry of a cylindrical tube as a simplified model of bone [10, 11]. Since the distribution of stress and locations of stress concentration are affected by geometry, the FE model geometry should be of a human long bone to improve the ability of the model to predict torsional fracture.

To our knowledge, the effect of transverse bicortical holes in the human tibia subjected to torsional loading has not been examined. The objective of the current study was to develop a FE

model and compare it to an experimental model of a composite analogue distal tibia with bicortical holes in torsion.

Methodology

This study was conducted with two models: an experimental model and a FE model. For the experimental model, composite analogue distal human tibiae were tested in torsion to failure. The FE model was developed using the geometry of a composite analogue tibia, and the boundary conditions and loads applied were based on the interpretation of the experimental model.

Experimental Model

The middle-third section of six fourth-generation composite analogue left tibiae (model #3402, Pacific Research Laboratories, Inc., Vashon, WA) were tested in torsion to fracture (Figure 1a). Three bicortical screw holes were introduced to simulate *in vivo* removal of orthopedic screws. A custom jig was used to standardize the drill positions, and a 6-hole 4.5 mm orthopedic plate was used as a template to drill three pilot holes for the screws. A 4.5 mm self-tapping AO cortical screw was then inserted and removed from each pilot hole.

The specimens were proximally and distally locked with dental cement (CAD-scan, Garreco Incorporated, Heber Springs, AR) in custom holding fixtures with an exposed length of 85 mm (Figure 1b). The holding fixtures were positioned and secured onto the actuator of the MTS Bionix servohydraulic materials testing system (MTS Model 858, Eden Prairie, MN), and the intramedullary shaft was carefully aligned with the rotational axis of the MTS machine. A compressive load of 15 N, under load control, was applied axially to each specimen, and then torque was applied from 0 Nm to complete structural failure at a loading rate of 0.25 degrees per second. The 15 N axial compressive load was applied to stabilize the test specimen and fixture before applying torque. Testing was initiated with three preconditioning torque cycles from 0 Nm to 15 Nm at 0.25 degrees per second, and then the load was applied continuously until failure occurred. Rotation angle and torque were collected every 0.1 seconds, and the average specific torsional stiffness was calculated as the torque-rotation slope (range: 15.3 Nm to 17.3 Nm) multiplied by the specimen's exposed length (range: 0.080 m to 0.090 m).

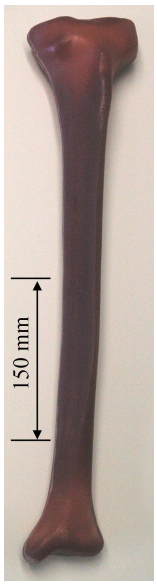

(a)

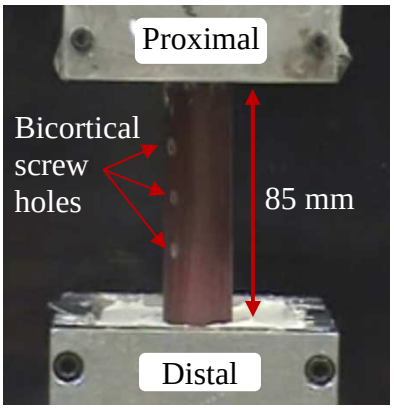

(b)

Figure 1. Experimental model. (a) Section of analogue tibia tested (b) Experimental setup

FE Model

The CAD geometry, shown in Figure 2, was of the distal portion of a fourth-generation composite analogue tibia (model #3402) with three equally spaced, transverse, bicortical holes. The holes were modeled as drill holes, omitting the screw threads, and they had the average diameter of the orthopedic screws, 3.75 mm. Screw threads were omitted to reduce model complexity and analysis time, and this approach has been used in previous studies [9, 11, 12]. The cancellous bone was also omitted based on former research [13].

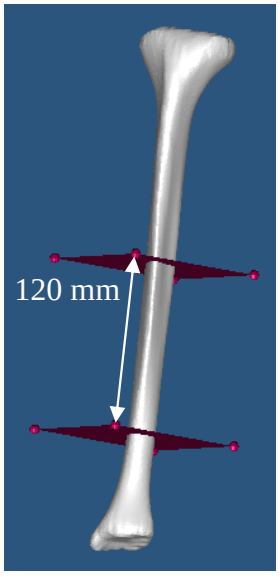

(a)

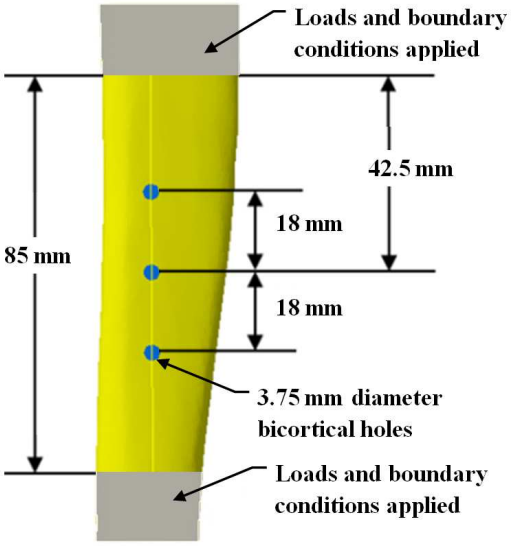

(b)

Figure 2. FE model. (a) Section of the distal tibia modeled (b) Position of the transverse drill holes

The FE model was developed in Altair HyperMesh, processed with Altair RADIOSS, and post-processed in Altair HyperView. The mesh contained solid twenty-node brick elements with an element size of 1 mm. The thinnest sections of the cortical wall had at least five elements in the thickness. The model contained 35,355 elements and 164,794 nodes.

An isotropic linear elastic material model was used to simulate the composite analogue tibia. This material model is commonly used for FE model comparisons and studies on long bones [9, 14, 15, 16, 17]. The properties used to define the linear elastic material include Young's modulus (10.1 GPa), density (1.64×10^{-6} kg/mm^3), and Poisson's ratio (0.3). The modulus and density were provided by the manufacturer [18], and Poisson's ratio was assigned to be consistent with former composite long bone FE models [13, 14, 19].

Boundary conditions and loads were applied to the nodes on the outer surfaces of the proximal and distal ends of the tibia section, as shown in Figure 3. The distal end of the model was fixed and the proximal end was rotated (2.5 deg/ms) clockwise, simulating an external twist, about the mechanical axis of the tibia. Similar to the experimental model, a 15N axial compressive load was applied prior to initiating rotation. The axial load and rotation were applied with a ramp and then held constant. Constraints were applied to the proximal end to allow only axial translation and rotation about the mechanical axis of the tibia.

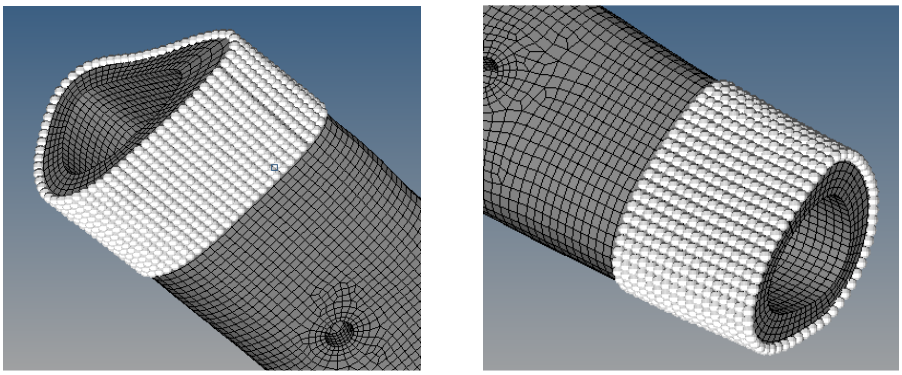

(a) Proximal End (b) Distal End

Figure 3. Nodes subjected to loading, rotation, and/or constraints.

The FE model was evaluated at two time points: 1) at the rotation angle of fracture determined by the experimental model, and 2) at the composite's maximum stress limitation. Table 1 shows the maximum stress limitations in tension, compression, and shear of the composite material simulating cortical bone in the fourth-generation composite analogue tibia. The time point at which the FE model first reaches the composite maximum stress limit, is viewed as an indication of initial micro-crack formation, rather than as an indication of component failure.

TABLE 1. STRESS LIMITS OF THE ANALOGUE CORTICAL BONE COMPOSITE MATERIAL [18]

Stress	**Maximum (MPa)**
Tension	106.0
Compression	157.0
Shear	93.2

Results

Table 2 lists the fracture torque, angle of rotation at fracture, and specific torsional stiffness of both the experimental and FE models, and Figure 4 is a plot of the torque versus rotation angle of the models. When the FE model reached the angle of rotation at which experimental fracture occurred, the torque was 4% less than the experimental model and was within the standard deviation of the experimental model's fracture torque. Also at this angle of rotation, 6.1% of the elements exceeded the maximum stress limitations of the composite analogue cortical bone. The FE model reached the stress limitations of the composite material at a torque 54% lower than the fracture torque of the experimental model and a rotation angle 52% lower than the fracture angle of the experimental model. The tensile limit was reached prior to exceeding the compressive and shear limits. The specific torsional stiffness of the FE model was 23% less than the experimental model.

TABLE 2. SUMMARY OF RESULTS

Model Description		**Torque (Nm)**	**Rotation (Degrees)**	**Specific Torsional Stiffness (Nm^2/deg)**
Experimental model at fracture		127.2 $\pm$ 7.1	9.6 $\pm$ 0.3	1.41 $\pm$ 0.09
FE model	At rotation angle of experimental fracture	122.1	9.6	1.08
	At composite material's maximum stress limits	58.8	4.6	1.08

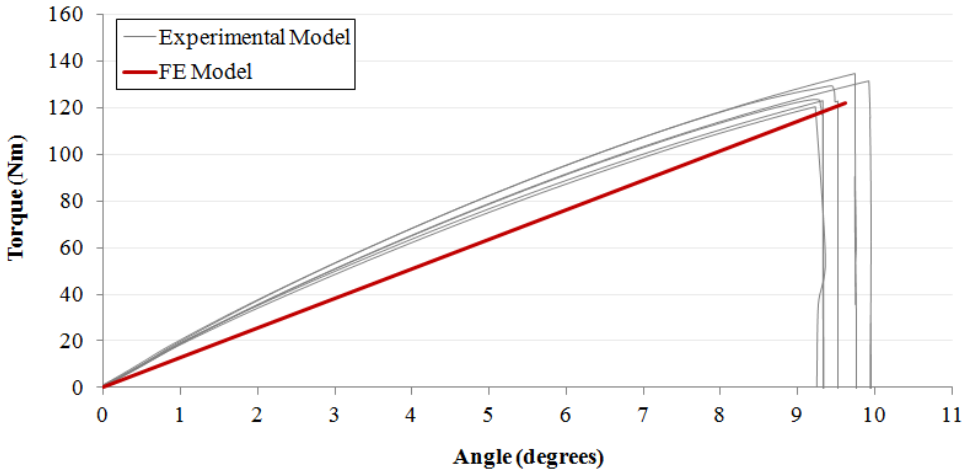

Figure 4. Torque versus angle plot of the experimental and FE models

Contours of major principal stress, minor principal stress, and maximum shear stress are shown in Figures 5, 6, and 7 respectively. In these contours, the two time points are pictured to show the development of stress, and the areas that are dark red-orange or red have exceeded the stress limitations of the composite cortical bone.

The drill holes deformed under the torsional loading, and locations of high stress concentrations developed around their edges. As shown in the contours, major principal stress (tension) concentrations occurred at an angle of 45 degrees around the holes, and shear stress concentrations occurred in the transverse and vertical directions. As anticipated, the minor principal stress (compression) was a mirror image of the major principal stress and was concentrated at an angle of negative 45 degrees around the holes.

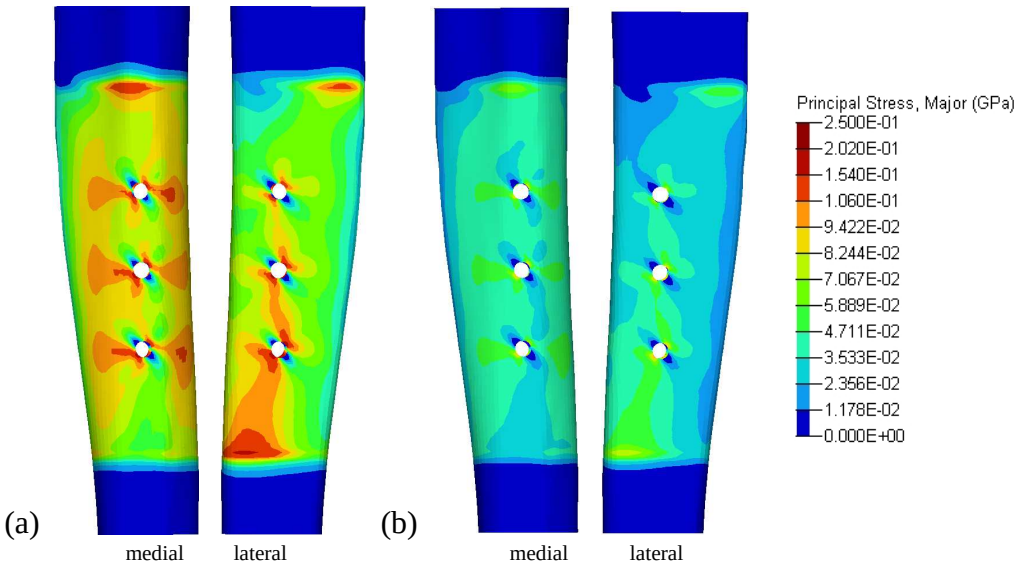

Figure 5. Major principal stress contours at (a) the fracture rotation angle determined by experiment and (b) the stress limits of the composite material.

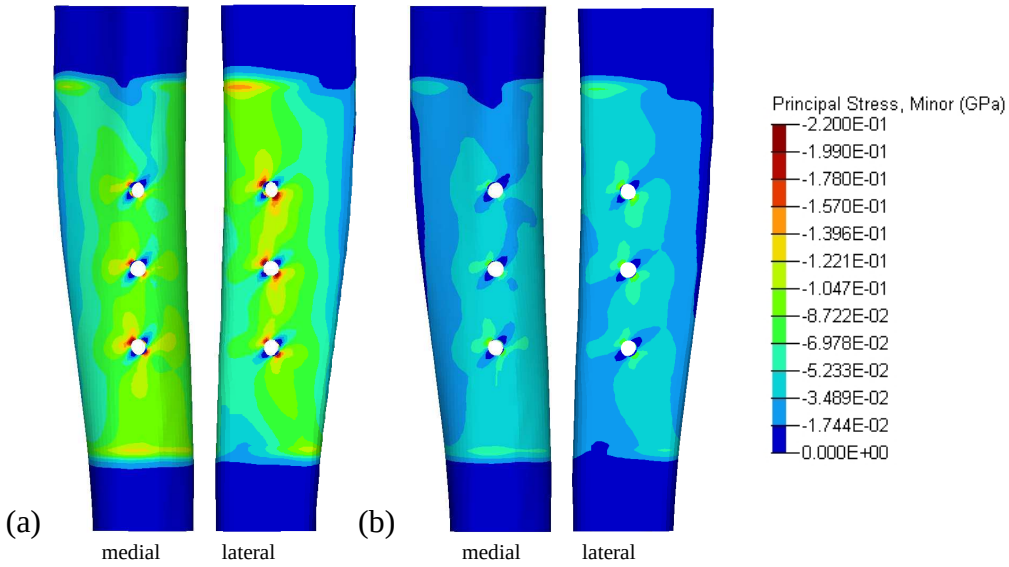

Figure 6. Minor principal stress contours at (a) the fracture rotation angle determined by experiment and (b) the stress limits of the composite material.

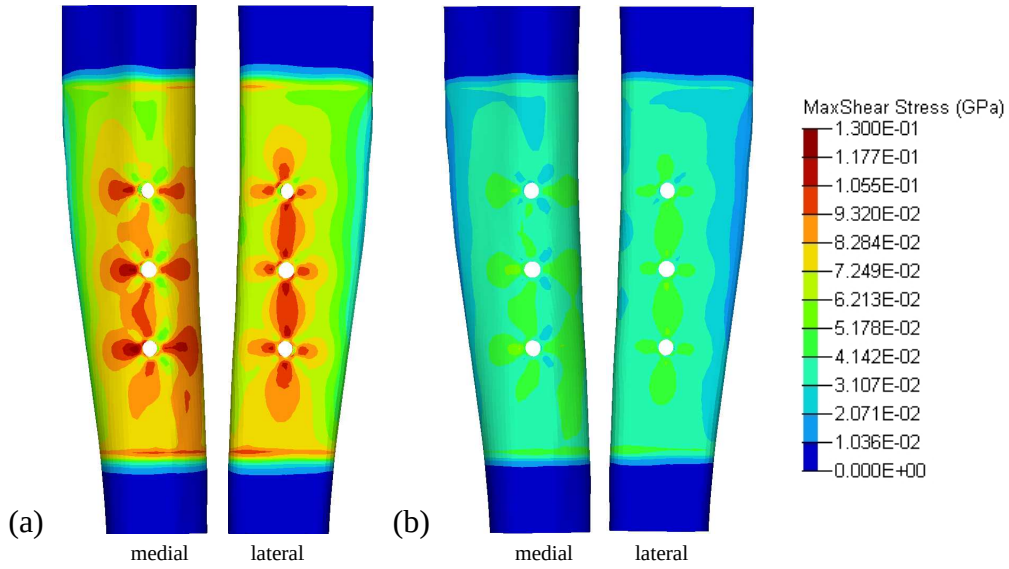

Figure 7. Maximum shear stress contours at (a) the fracture rotation angle determined by experiment and (b) the stress limits of the composite material.

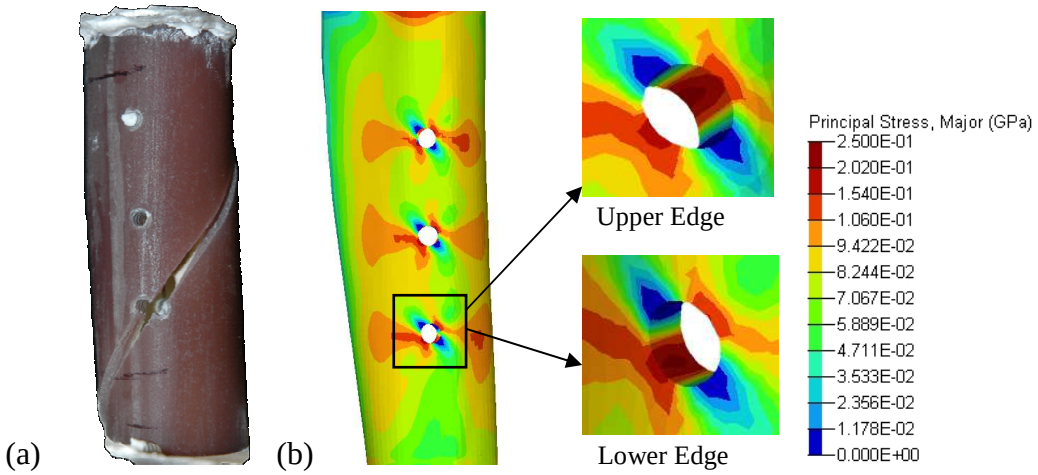

Figure 8. Fracture path comparison of (a) experimental analogue tibia specimen and (b) FE model major principal stress contour.

When loaded in torsion, long bones fail on a plane at 45 degrees to the loading axis [20, 21]. This is the plane of maximum tensile stress; therefore, the major principal stress contour is the best indicator for potential fracture sites. Figure 8 compares this stress contour with an experimental specimen fracture, which initiated at a 45 degree angle through the lower hole on the medial surface. In the FE model, the major principal stress concentrations were highest at a 45 degree angle around this same hole. Furthermore, the principal stress was higher on the upper inside edge of this hole than on the lower edge.

Discussion

To our knowledge, this is the first study to evaluate the torsional strength of a composite analogue tibia with bicortical holes using both experimental and FE models. In this study, the tibia was selected because 1) tibial shaft fractures are common injuries that occur after falls, car accidents, sports injuries, and other activities, 2) plates and screws are commonly used for fracture fixation of the tibia, and 3) the tibia, in comparison to other long bones, is subjected to more pure torsional loads, rather than combination loading (bending, compression, tension). Furthermore, an analogue tibia was used to reduce variability between specimens and allow examination of essentially anatomically identical specimens. Cadaveric specimens, on the other hand, vary widely not only in their geometry but also in their bone density and tissue properties, which are affected by disease and aging. According to the available literature, the fourth-generation analogue models fall within the published physiological range of average healthy adult bones (age: <80 years old) [22, 23, 24, 25, 26].

There are limitations to the models. Firstly, over time, bone in the clinical situation is known to remodel and fill screw holes after orthopedic hardware removal. The experimental and FE models can only validate the clinical situation in regards to fresh holes. Secondly, only cortical bone was simulated in the FE model, while the experimental model had two materials to represent the bone tissues: short fiber filled epoxy for cortical bone and rigid polyurethane foam for cancellous bone. Papini *et al*. [13] found that omitting the cancellous bone from a

computational model resulted in axial and torsional stiffness within 1% of those obtained when modeling both the cancellous and cortical bone due to the fact that the modulus of cancellous bone was more than an order of magnitude smaller than that of cortical bone. Since the elastic modulus of the two analogue bone materials were two orders of magnitude different, omission of the cancellous bone from the FE model did not significantly affect the results. Thirdly, the experimental model contained screw holes, while the FE model contained drill holes. Cortical screws were inserted and removed from the experimental specimens, and the impressions left by the screw threads create potential sites for fracture initiation [27]. In a FE model, small features such as screw threads reduce element size and increase analysis time. Therefore, screw threads were omitted, and holes with an average diameter of the cortical screws were modeled. Former research related to holes in bones subjected to torsion also simplified FE models by omitting screw threads [9, 11, 12].

There are also limitations within the FE material model which attributed to differences between the FE and experimental models. The specific torsional stiffness of the FE model is lower than the experimental model because the FE material model only uses one modulus and does not account for both the transverse and tensile moduli of the composite. Both shear and tension play a significant role in the simulation, and although the failure mode was in tension, the transverse modulus was used because of the torsional loading. With the transverse modulus being 37% lower than the tensile modulus, omission of the tensile modulus resulted in a low torsional stiffness, which did not mimic the torsional stiffness of the experimental model. Furthermore, the linear material model does not simulate yielding, which the experimental analogue tibia demonstrated with the gradual decline in stiffness with increased torsion. Without yielding the stress levels increased at an artificially high rate, which contributed to the FE model reaching the stress limitations at a relatively low torque in comparison to the experimental fracture torque. Considering future use of the FE model, material properties simulating human bone would be more useful than properties simulating analogue bone. Therefore, further development of the composite material model was not pursued, and the incorporation of a material model simulating human bone was reserved for a future study.

Locations of stress concentrations are well predicted by the FE model and thus, potential fracture sites can be identified. During the experiment, the analogue tibia fractured along a helix at an angle of 45 degrees passing through the lower hole on the medial surface. The FE model predicted the same fracture site as the experimental model, and further determined that the fracture would initiate on the upper inside edge of this hole. In both the experimental and FE models, the locations of the stress concentrations around the holes were consistent with the findings of Kuo *et al*. [11], which show that fractures in tubes having a single-cortex hole of small defect ratios, 10-40%, propagate along a helix with an angle of 45 degrees. The defect ratio of the FE model (16%) was within this range, and high stress concentrations around the holes were at the predicted angle of 45 degrees.

Conclusion

A finite element computer model of an analogue tibia with bicortical holes simulated an experimental torsional fracture test and successfully predicted the location of initial fracture and the fracture torque within the standard deviation of experimental results. For further advancement of the model, material properties representing human bone can be incorporated,

and results can be compared to those obtained with human cadaveric specimens. Further studies could utilize this model to investigate variables such as bone quality, hole size, hole shape, spacing between holes, and direction of rotation. Additionally, this model could be compared to a cylindrical tube model to see how geometric simplification affects the torsional response.

Acknowledgements

The authors thank Altair applications engineer Mark Virginia for assisting this study with exceptional technical support.

List of Figures

List of Tables

References

[1] Anderson LD, Sisk D, Tooms RE, and Park W 3rd. 1975. "Compression-plate fixation in acute diaphyseal fractures of the radius and ulna." *Journal of Bone and Joint Surgery American*. 57(3):287-297.

[2] Hidaka S, and Gustilo RB. 1984. "Refracture of bones of the forearm after plate removal." *Journal of Bone and Joint Surgery American.* 66(8):1241-1243.

[3] Mih AD, Cooney WP, Idler RS, and Lewallen DG. 1994. "Long-term follow-up of forearm bone diaphyseal plating." *Clinical Orthopaedics and Related Research*. 299:256-258.

[4] Tonino AJ, Davidson CL, Klopper PJ, and Linclau LA. 1976. "Protection from stress in bone and its effects: experiments with stainless steel and plastic plates in dogs." *Bone & Joint Surgery*. 58(B):107-113.

[5] Moyen BJ-L, Labey PJ Jr, Weinberg EH, and Harris WH. 1978. "Effects on intact femora of dogs of the application and removal of metal plates." *Bone & Joint Surgery*. 60(A):940-947.

[6] Rosson J, Egan J, and Shearer J. 1991. "Bone Weakness after the Removal of Plates and Screws. Cortical Atrophy or Screw Holes." *Bone & Joint Surgery*. 73(2):283-286.

[7] Clark CR, Morgan C, Sonstegard DA, and Matthews LS. 1977. "The Effect of Biopsy-Hole Shape and Size on Bone Strength." *Bone & Joint Surgery*. 59(2):213-217.

[8] Edgerton BC, Morrey BF, and An KN. 1990. "Torsional Strength Reduction due to Cortical Defects in Bone." *Orthopaedic Research.* 8(6):851-855.

[9] Reminger a, Miclau T, and Lindsey R. 1997. "The Torsional Strenght of Bones with Residual Screw Holes from Plates with Unicortical and Biocortical Purchase." *Clinical Biomechanics*. 12(1):71:73.

[10] Hipp JA, Edgerton BC, An KN, and Hayes WC. 1990. "Structual Consequensces of Transcortical Holes in Long Bones Loaded in Torsion." *Biomechanics.* 23(12):1261-1268.

[11] Kuo RF, Chao EYS, Rim K, and Park JB. 1991. "The Effect of Defect Size on the Stress Concentration and Fracture Characteristics for a Tubular Torsional Model with a Transverse Hole." *Biomechanics.* 24(2):147-155.

[12] Cheung G, Zalzal P, Bhandari M, Spelt JK, and Papini M. 2004. "Finite Element Analysis of a Femoral Retrograde Intramedullary Nail Subject to Gait Loading." *Medical Engineering & Physics*. 26(2):93-108.

[13] Papini M, Zdero R, Schemitsch EH, and Zalzal P. 2007. "The Biomechanics of Human Femurs in Axial and Torsional Loading: Comparison of Finite Element Analysis, Human Cadaveric Femurs, and Synthetic Femurs." *Biomechanical Engineering*. 129(1):12-19.

[14] Completo A, Fonseca F, and Simoes JA. 2007. "Finite Element Experimental Cortex Strains of the Intact and Implanted Tibia." *Biomechanical Engineering*. 129(5):791-797.

[15] Keyak JH, and Rossi S. 2000. “Prediction of Femoral Fracture Load using Finite Element Models: An Examination of Stress- and Strain- Based Failure Theories.” *Biomechanics.* 33(2): 209-214.

[16] Lotz JC, Cheal, EJ, and Hayes WC 1991. “Fracture Prediction for the Proximal Femur Using Finite Element Models: Part I – Linear Anaysis.” *Biomechanical Engineering.* 113(4):353-360.

[17] Beillas P, Lee SW, Tashman S, and Yang KH. 2007. “Sensitivity of Tibio-femoral Response to Finite Element Modeling Parameters.” *Computer Methods in Biomechanics and* Biomedical Engineering. 10(3):209-221.

[18] Pacific Research Laboratories, Inc., Vashon, Washongton. Composite Bones. (Retrieved 2012). http://www.sawbones.com/products/bio/composite.aspx.

[19] Gray HA, Zavatsky AB, Taddei F, Cristofolini L, and Gill HS. 2007. “Experimental Validation of a Finite Element Model of a Composite Tibia.” *Proceedings of the Institution of Mechanical Engineers.* 221(3):315-324.

[20] Brooks DB, Burstein AH, and Frankel VH. 1970. "The biomechanics of torsional fractures: the stress concentration effect of a drill hole." *Journal of Bone and Joint Surgery American.* 52(A):507-514.

[21] Peterson DL, Skraba JS, Moran JM, and Greenwald AS. 1984. "Fracture of long bone: rate effects under singular and combined loading states." *Journal of Orthopaedic Research*. 1:244-250.

[22] Cristofolini L, and Viceconti M. 2000. "Mechanical Validation of Whole Bone Composite Tibia Models." *J Biomech*. 33(3):279-288.

[23] Cristofolini L, Viceconti M, Cappello A, and Toni A. 1996. "Mechanical Validation of Whole Bone Composite Femur Models." *J Biomech*. 29(4):525-535.

[24] Heiner AD. 2008. "Structural Properties of Fourth-Generation Composite Femurs and Tibias." *J Biomech*. 41(15):3282-3284.

[25] Heiner AD, and Brown TD. 2001. “Structural Properties of a New Design of Composite Replicate Femurs and Tibias.” *Biomechanics.* 34(6):773-781.

[26] Gardner MP, Chong AC, Pollock AG, and Wooley PH. 2010. “Mechanical Evaluation of Large-Size Fourth-Generation Composite Femur and Tibia Models.” *Ann Biomed Eng*. 38(3):613-20.

[27] Malone CB, Heiple KG, and Burstein AH. 1977. “Bone Strength: Before and After Removal of Unthreaded and Threaded Pin and Screw.” *Clinical Orthopaedics & Related Research.* 123:259-260.